Triple-Pomeron couplings in dual models

J.-P. Ader

Laboratoire de Physique Théorique, Université de Bordeaux I, 33170 Gradignan, France*

L. Clavelli

Center for Theoretical Physics, Department of Physics and Astronomy, University of Maryland, College Park, Maryland 20742
(Received 10 April 1978)

By examining the dual amplitudes for external Pomerons in the triple-Regge region, we extract the triple-Pomeron couplings $g_{PPP}(t)$ corresponding to the dual models of Veneziano and of Neveu and Schwarz. We also verify the expected central region plateau in Pomeron production and isolate the $p_\perp$ dependence.

I. INTRODUCTION

In the Reggeon calculus, the coupling between three Pomerons plays a basic role. It was shown very early by Gribov and Migdal[1] that a weak-coupling solution of the calculus requires the vanishing of the coupling in the forward direction. Gribov's triple vertex is closely related to the triple-Pomeron coupling of inclusive reactions.[2] There it can be shown, most clearly through the use of the inclusive sum rules that the triple-Pomeron coupling must vanish at $t = 0$ if the total cross sections are to approach a constant asymptotically.

For a number of years around 1970 the vanishing of the triple-Pomeron coupling was almost axiomatic and dynamical models for this behavior were eagerly sought. With cross sections growing in the present energy regime and the renormalization group suggesting a strong-coupling solution[3] to the Reggeon calculus, the vanishing of the triple-Pomeron coupling is no longer taken for granted. Experimentally also, there are at present no indications of such a vanishing.

For this reason and because of its basic importance to the Reggeon calculus, it is interesting to study the triple coupling and its t dependence in a semirealistic, resonant amplitude with Regge behavior such as provided by any of the dual-resonance models.

The inclusive cross section $a + b \rightarrow c + X$ is proportional to the missing-mass discontinuity of the six-point function $a + b + \bar{c} \rightarrow a + b + \bar{c}$ in the forward direction. The triple-Regge regime is obtained when the invariant energy in the ab channel is much greater than the missing mass which is itself much greater than the Regge scale, say 1 GeV. In this limit a six-point function with Regge behavior and appropriate analyticity satisfies

$$\lim_{\substack{M^2 \to \infty \\ s/M^2 \to \infty}} \mathrm{Disc} A_6 \sim \sum_{i,j,k} (s/M^2)^{\alpha_i(t) + \alpha_j(t)}$$
$$\times [\alpha(M^2)]^{\alpha_k(0)} g_{ikj}(t). \quad (1.1)$$

Clearly the highest-lying trajectory will dominate the sum and hence the importance of the triple-Pomeron coupling. This behavior is depicted by the Reggeon graph of Fig. 1. As defined here, the triple vertex $g_{ikj}(t)$ contains not only the triple-Regge vertex proper, but also Reggeon propagator and residue functions which can be factored out, if one wishes, through knowledge of the elastic scattering.

This triple-Regge behavior in a dual amplitude was first confirmed in a study of the Veneziano-model Born term contribution to the six-point function.[4] The tree graphs in a dual model contain only secondary trajectories dual to resonances and no diffractive effects. The result of Ref. 4 is therefore a statement of the triple coupling of Eq. (1.1) with i, j, k corresponding to any of the leading ρ, f, ω, A_2 trajectories. These are all related by isospin and exchange degeneracy to the one result,

$$g_{fff}(t) = 2\pi g^4 \frac{\Gamma^2(-\tfrac{1}{2}\alpha_f(t))}{\Gamma^2(\tfrac{1}{2}[1 + \alpha_f(t)])} \frac{4^{-\alpha_f(t)}}{\Gamma(1 + \alpha_f(0) - 2\alpha_f(t))} .$$

$$(1.2)$$

Here g is the coupling constant of the dual perturbation expansion which gives the deviation from zero-width resonances through loop corrections. One might take g, therefore, as proportional to
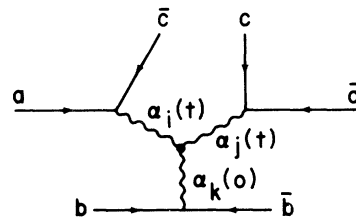
FIG. 1. Triple-Regge graph for the process $a + b \rightarrow c$ + anything.
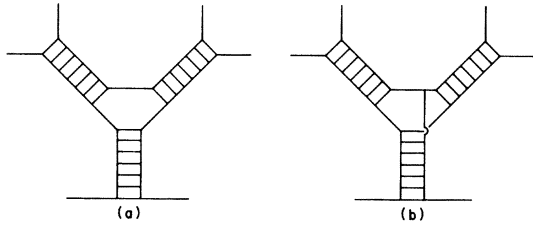
FIG. 2. Ladder graphs in ϕ^3 field theory showing triple-Regge behavior with (a) planar coupling and (b) nonplanar coupling.

the typical width of a resonance relative to a typical mass or Regge scale.

It was observed from this expression that if the intercept of the f trajectory was unity, as is that of the Pomeron, the triple coupling would vanish at $t = 0$ due to the last Γ function in the denominator of (1.2). A similar zero was found in calculating the planar ϕ^3 ladder graphs of Fig. 2(a) in the triple-Regge region.[5] This suggested that the inverse Γ function of (1.2) might be a very general result leading to the vanishing at $t = 0$ of the triple coupling of an intercept 1 trajectory. However, a subsequent calculation[6] of ϕ^3 ladder graphs with the nonplanar connection of Fig. 2(b) gave instead of the inverse Γ of Eq. (1.2) a factor $\sin\{\frac{1}{2}\pi[2\alpha(t) - \alpha_0]\}$ which does not vanish at $t = 0$ for an intercept-1 trajectory. Since the Pomeron is thought to be associated with nonplanar couplings the result of Eq. (1.2) is not a convincing model for the vanishing of $g_{PPP}(0)$.

The actual triple-Pomeron coupling of the dual model is given by the discontinuity of the two-loop graph shown in Fig. 3. Because of its complexity this diagram has never been studied in the appropriate depth. Extrapolating somewhat from single-Pomeron results, Lovelace[7] argued that the triple-Pomeron coupling would be nonzero in the Veneziano model but would vanish in the Neveu-Schwarz model (NSM) owing to the fermionic internal structure of the latter.
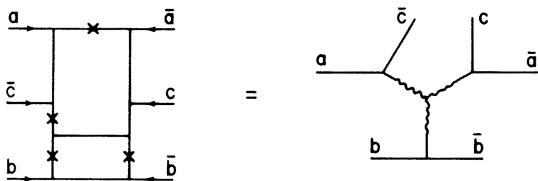
FIG. 3. Two-loop duality graph containing the triple-Pomeron coupling. Wavy lines represent Pomerons, straight lines represent Reggeons. The effect of the twists is to prevent particles separated by a Pomeron from exchanging quarks.

The graph of Fig. 3 represents a nine-dimensional integral in dual models complicated by the presence of Regge-Regge cuts in Pomeron cross channels. We observe, however, that the relevant information can be simply extracted from the dual amplitudes with external Pomerons. In the Veneziano model these are the amplitudes of Virasoro and Shapiro[8] while, for the Neveu-Schwarz model, the corresponding Pomeron amplitudes were given by Schwarz[9] and by Aldrovandi and Neveu.[10] The relevant integrals are only six dimensional and contain no Regge cuts since in the scattering of Pomerons, the Pomeron trajectory is dual to Pomeron resonances.

In Secs. II and III of this article we extract the triple-Pomeron coupling of the Veneziano model and the Neveu-Schwarz model, respectively. By supplying the Pomeron residue functions known from the four-point twisted loop we are able to give the contribution of the two-loop graph of Fig. 3 to the triple-Regge region. In Sec. IV we examine the Pomeron six-point function in the central region $t, u \to -\infty$ with $tu/s = \mu^2 + P_\perp^2$ fixed. This "pomeronization" is of possible interest for the following reasons:

(a) The existence of quarkless, Pomeronic resonances is a firm prediction of the dual perturbation expansion. They correspond to the hypothetical color-singlet gluon bound states of color gauge theory. The experimental searches for such states depend on the prediction of distinctive features in their decay or their production amplitudes. For example the Pomeron states are expected to be significantly more narrow than quark bound states because the decay of a Pomeron is higher order in g, the dual coupling constant. Similarly, if there were theoretical reasons to expect the production of Pomerons to be enhanced relative to normal particles in some kinematical region such as at high $P_\perp$, this could be of experimental importance.

(b) The production of Pomerons in the central region could shed light on the topologically similar but more complicated dual integral for the production of normal particles in the double-Pomeron limit. We have recently proposed a Regge-cut model[11] for particle production based on the assumption that multi-Pomeron exchange in the central region would cause a shallower $P_\perp$ dependence than the dual Born term because of the smaller slope of the Pomeron trajectory. The first indication of this could come in a study of the $P_\perp$ dependence of Pomeron production. In the present article we demonstrate the central-region plateau and scaling behavior for Pomeron production and determine the asymptotic form of the $P_\perp$ dependence.

In Sec. V we conclude with a discussion of our results and a prognosis.

II. $g_{PPP}\,(t)$ IN THE VENEZIANO MODEL

To extract the triple-Pomeron coupling in the Veneziano model we begin with the Shapiro-Virasoro amplitude corresponding to the graph of Fig. 4 for six external Pomeron ground states. The missing-mass discontinuity of this amplitude gives the inclusive cross section for $a+b \to c+X$. The kinematics are given by

$$t = -\,(k_a + k_{\overline{c}})^2, \quad \overline{t} = -\,(k_{\overline{a}} + k_c)^2\,, \tag{2.1a}$$
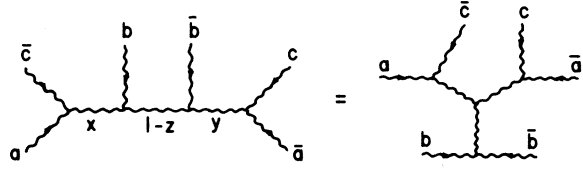
FIG. 4. Tree graph for external Pomerons allowing extraction by factorization of the triple-Pomeron coupling.

$$u = -\,(k_b + k_{\overline{c}})^2, \quad \overline{u} = -\,(k_{\overline{b}} + k_c)^2\,, \tag{2.1b}$$

$$s = -\,(k_a + k_b)^2, \quad \overline{s} = -\,(k_{\overline{a}} + k_{\overline{b}})^2\,, \tag{2.1c}$$

The discontinuity is to be taken across the positive M^2 cut with u, s and $\overline{u}, \overline{s}$ continued to the real axis from complex-conjugate positions.[12] Since t is not taken asymptotic we can safely identify t and $\overline{t}$. The missing mass squared is $M^2 = t + u + s$, and in terms of these variables the amplitude of Fig. 4 is

$$A_6 = g^8 \int\ d^2x\ d^2y\ d^2z\,|xy|^{-\alpha(t)-2}\,|z|^{-\alpha_0-2}|1-z|^{-\alpha(M^2)-2}$$

$$\times |1-x|^{-\alpha(u)-2}|1-y|^{-\alpha(\overline{u})-2}\,|1-y(1-z)|^{\alpha(\overline{u})+2}|1-x(1-z)|^{\alpha(u)+2}|1-xy(1-z)|^{-\alpha_0-2}\,. \tag{2.2}$$

The integrals are taken over the entire complex plane and the amplitude for large s and u and physical t and α_0 is the analytic continuation from the region of imaginary s and u and negative $\alpha(t)$, α_0. All of the trajectory functions in (2.2) are Pomeron trajectories and the graph is of order g^8 since in a dual model the Pomeron interacts with the square of the Born-term coupling constant. In the triple-Pomeron region $\alpha(t) < 1 \ll \alpha(M^2) \ll \alpha(s)$. Therefore, we may write to a good approximation $u = -s$, $\overline{u} = -\overline{s}$.

In the limit of asymptotic M^2, s, and $\overline{s}$, the dominant contribution to A_6 comes from the region near x, $y, z = 0$. Expanding, therefore, around these points we have

$$A_6 = g^8 \int\ d^2x\ d^2y\ d^2z\,|xy|^{-\alpha(t)-2}\,|z|^{-\alpha_0-2}e^{\alpha(M^2)\mathrm{Re}\,z}\,e^{-\alpha(s)\mathrm{Re}\,x}\,e^{-\alpha(\overline{s})\mathrm{Re}\,y}\,. \tag{2.3}$$

The integral splits into three factors with the substitution

$$x = x'/z\,, \quad y = y'/z\,,$$

$$A_6 = g^8 \int\ d^2z\,|z|^{2\alpha(t)-\alpha_0-2}\,e^{\alpha(M^2)\mathrm{Re}\,z}\int\ d^2x'\,|x'|^{-\alpha(t)-2}e^{-\alpha(s)\mathrm{Re}\,x'}\int\ d^2y'\,|y'|^{-\alpha(t)-2}e^{-\alpha(\overline{s})\mathrm{Re}\,y'}\,. \tag{2.4}$$

Let us examine the first factor

$$I_1 = \int\ d^2z\,|z|^{2\alpha(t)-\alpha_0-2}e^{\alpha(M^2)\mathrm{Re}\,z}$$

$$= \Gamma(2\alpha(t)-\alpha_0)\int_0^{2\pi}\ d\theta\,[-\alpha(M^2)\cos\theta]^{\alpha_0-2\alpha(t)}\,. \tag{2.5}$$

The missing mass squared may now be continued to the positive real axis and the discontinuity is seen to come from the region of positive $\cos\theta$,

$$\mathrm{Disc}\,I_1 = \Gamma(2\alpha(t)-\alpha_0)\sin\pi[2\alpha(t)-\alpha_0]\int_{-\pi/2}^{\pi/2}\ d\theta\,[\alpha(M^2)\cos\theta]^{\alpha_0-2\alpha(t)}$$

$$= \frac{\pi}{\Gamma(1+\alpha_0-2\alpha(t))}\,[\alpha(M^2)]^{\alpha_0-2\alpha(t)}\,B\left(\frac{\alpha_0+1-2\alpha(t)}{2},\frac{1}{2}\right)\,. \tag{2.6}$$

Using the doubling formula for the Γ function this can be written

$$\text{Disc}I_1 = \frac{\pi^2 2^{2\alpha(t) - \alpha_0}[\alpha(M^2)]^{\alpha_0 - 2\alpha(t)}}{\Gamma^2(\frac{1}{2}[2 + \alpha_0 - 2\alpha(t)])} \ . \tag{2.7}$$

The remaining two factors in (2.4) are, after performing the integrations over the magnitudes of x' and y',

$$I_2 I_3 = \Gamma^2(-\alpha(t)) \int_0^{2\pi} d\phi \, d\omega [\alpha(s)\cos\phi]^{\alpha(t)}[\alpha(\bar{s})\cos\omega]^{\alpha(t)} \ . \tag{2.8}$$

Since $\alpha(s)$ and $\alpha(\bar{s})$ occupy complex-conjugate positions in the complex plane, the phases are defined by $I_2 = I_3^*$. That is

$$I_2 I_3 = \Gamma^2(-\alpha(t)) \int_{-\pi/2}^{\pi/2} d\phi \, d\omega [\alpha(s)\alpha(\bar{s})\cos\phi \cos\omega]^{\alpha(t)}(1 + e^{i\pi\alpha(t)})(1 + e^{-i\pi\alpha(t)})$$

$$= \frac{\Gamma^2(-\frac{1}{2}\alpha(t))}{\Gamma^2(1 + \frac{1}{2}\alpha(t))} 4^{-\alpha(t)} \pi^2 [\alpha(s)]^{2\alpha(t)} \ , \tag{2.9}$$

where in the last step we take the limit of $\alpha(s)$ and $\alpha(\bar{s})$ to the real axis. Putting together the three factors I, I_2, I_3 we have

$$\text{Disc}A_6 = g^8[\alpha(s)/\alpha(M^2)]^{2\alpha(t)} \frac{[\alpha(M^2)]^{\alpha_0}\pi^4 2^{-\alpha_0}\Gamma^2(-\frac{1}{2}\alpha(t))}{\Gamma^2(1 + \frac{1}{2}\alpha(t))\Gamma^2(\frac{1}{2}[2 + \alpha_0 - 2\alpha(t)])} \ . \tag{2.10}$$

Comparing with (1.1) we can extract the triple coupling for the graph of Fig. 4. Eliminating the two Pomeron propagators and six powers of the coupling constant gives us for the triple-vertex proper

$$\tilde{g}_{PPP}(t) = \frac{g^2\pi^4 2^{-\alpha_0}}{\Gamma^2(\frac{1}{2}[2 + \alpha_0 - 2\alpha(t)])} \ . \tag{2.11}$$

If α_0, the Pomeron intercept, is 1, $g_{PPP}(0)$ is nonvanishing. From (2.10) it is a simple matter to write down the asymptotic behavior of the discontinuity of the two-loop graph, Fig. 3. It suffices to multiply (2.10) by the Pomeron form factors to the $a\bar{c}$, $\bar{a}c$, and $b\bar{b}$ states:

$$f_P(t) = B(\frac{1}{2}[\alpha_P(t) - \alpha_f(t)], \frac{1}{2}) 2^{\alpha_P(t) - \alpha_f(t) - 1} \ . \tag{2.12}$$

Thus,

$$\lim_{\substack{M^2 \to \infty \\ s/M^2 \to \infty}} \text{Disc}_{M^2} A_6^{2 \text{ loop}} \sim g^8[\alpha(s)/\alpha(M^2)]^{2\alpha_P(t)} \frac{[\alpha_P(M^2)]^{\alpha_P(0)}\pi^4 2^{-\alpha_P(0)}\Gamma^2(-\frac{1}{2}\alpha_P(t))}{\Gamma^2(1 + \frac{1}{2}\alpha_P(t))\Gamma^2(\frac{1}{2}[2 + \alpha_P(0) - 2\alpha_P(t)])} f_P^2(t)f_P(0) \ . \tag{2.13}$$

We turn now to the calculation of the same amplitude in the Neveu-Schwarz model, reserving further discussion of (2.13) for Sec. V.

III. $g_{PPP}(t)$ IN THE NEVEU-SCHWARZ MODEL

The vertex for ground-state Pomeron emission in the NSM differs from that of the Veneziano model by a product of the two anticommuting fields

$$\alpha_P' k \cdot H(z) k \cdot H'(z^*) = \alpha_P'\left(\sum_{m=0}^{\infty} (k \cdot b^{m\dagger}z^{m+1/2} + k \cdot b^m z^{-m-1/2})\right)\left(\sum_{m=0}^{\infty} (k \cdot b'^{m\dagger}z^{*m+1/2} + k \cdot b'^m z^{*-m-1/2})\right) , \tag{3.1}$$

where α_P' is the Pomeron trajectory slope. Therefore the six-Pomeron amplitude in the NSM is obtained by multiplying the integrand of (2.2) by

$$|1 - x|^2 |1 - y|^2 |z|^2 |1 - x(1 - z)|^{-2} |1 - y(1 - z)|^{-2} |1 - xy(1 - z)|^2 \, RR^* , \tag{3.2}$$

where

$$R = \alpha_P'^3 [xy(1-z)]^{1/2} \langle 0 | \, k_a \cdot b^0 \, k_{\bar c} \cdot H(1) k_b \cdot H(x) k_{\bar b} \cdot H(x(1-z)) k_c \cdot H(xy(1-z)) k_a \cdot b^{0\dagger} | 0 \rangle \ . \tag{3.3}$$

In the NSM with the critical dimension of space-time and in the ghost-free configuration, the Pomeron intercept is 2 and the Pomeron ground state is a scalar meson on the first daughter trajectory. Therefore,

$$\alpha_P' k_i k_j = -\tfrac{1}{2}\alpha_P(-(k_i + k_j)^2) \ . \tag{3.4}$$

In the NSM there are no tachyons on the leading Pomeron trajectory and this feature is retained if we extrapolate the model to the physical Pomeron intercept only after imposing (3.4).

We may perform all the contractions between fermionic oscillators required by (3.3) yielding, in the limit $u = -s$,

$$R = - 2^{-3}\alpha_P(s)^2(1-z)^{1/2} z \, [\alpha_P(t)(x-y)^2 + 2\alpha_P(0)xy] - 2^{-3}\alpha_P(0)\alpha_P(t)^2(1-z)^{1/2}/z$$

$$- 2^{-3}\alpha_P(0)[xy(1-z)^{1/2}/z][\alpha_P(t)^2 - \alpha_P(0)^2] \ . \tag{3.5}$$

Inserting (3.2) with (3.5) into the integrand of (2.2) the limit of asymptotic $\alpha(s)$, $\alpha(\bar s)$, and $\alpha(M^2)$ is again given by the region around $x, y, z = 0$. Thus all the factors in (3.2) except for $|z|^2 RR^*$ can be ignored. Furthermore, the first two factors in (3.5) become of comparable importance while the third is totally negligible. Exponentiating as in (2.3) we have

$$A_6^{NS} = 2^{-6} g^8 \int d^2x\, d^2y\, d^2z \, |xy|^{-\alpha(t)-2} |z|^{-\alpha_0 - 2} e^{\alpha(M^2)\text{Re}\, z} e^{-\alpha(s)\text{Re}\, x} e^{-\alpha(\bar s)\text{Re}\, y}$$

$$\times | \, \alpha(s)^2 z^2 [\alpha_P(t)(x-y)^2 + 2\alpha_P(0)xy] + \alpha_P(0)\alpha(t)^2 |^2 \ . \tag{3.6}$$

Again it is convenient to make the substitutions $x = x'/z$, y'/z. The z integral then factorizes and is given by (2.5) and (2.7). We have, therefore,

$$\text{Disc}_{M^2} A_6^{NS} = 2^{-6} g^8 \frac{\pi^2 2^{2\alpha(t) - \alpha_0}[\alpha(M^2)]^{\alpha_0 - 2\alpha(t)}}{\Gamma^2(\tfrac{1}{2}[2 + \alpha_0 - 2\alpha(t)])} \, J \ , \tag{3.7}$$

where J is the remaining integral over x' and y':

$$J \equiv \int d^2x\, d^2y \, |xy|^{-\alpha(t)-2} e^{-\alpha(s)\text{Re}\, x} e^{-\alpha(\bar s)\text{Re}\, y} \, | \, \alpha(s)^2[\alpha_P(t)(x-y)^2 + 2\alpha_P(0)xy] + \alpha_P(0)\alpha(t)^2 |^2 \ . \tag{3.8}$$

Integrating as in Sec. II we find

$$J = 64\pi^2 [\alpha(s)]^{2\alpha(t)} 4^{-\alpha(t)} \frac{\Gamma^2(1 - \tfrac{1}{2}\alpha(t))}{\Gamma^2(\tfrac{1}{2}\alpha(t))} \left[(2 - \alpha_0)^2 - \alpha_0(2 - \alpha_0) + \frac{\alpha_0^2}{4} \right] \ . \tag{3.9}$$

The first term in the large square brackets of (3.9) comes from the $|\alpha(s)|^4$ term in (3.8), the second term comes from the cross term in (3.8), and the third term derives from the $\alpha_P(0)^2 \alpha(t)^4$ in (3.8). If the Pomeron intercept is either 1 or 2, it is only this latter term that survives. Then (3.7) becomes

$$\text{Disc}_{M^2} A_6^{NS} = g^8 [\alpha(s)/\alpha(M^2)]^{2\alpha(t)} [\alpha(M^2)]^{\alpha_0} \pi^4 2^{-\alpha_0 - 2} \alpha_0^2 \Gamma^2(1 - \tfrac{1}{2}\alpha(t)) / \{\Gamma^2(\tfrac{1}{2}\alpha(t))\Gamma^2(\tfrac{1}{2}[2 + \alpha_0 - 2\alpha(t)])\}, \tag{3.10}$$

Eliminating the two Pomeron propagators and six powers of the coupling constant gives us again the triple-vertex proper:

$$g^{NS}_{PPP}(t) = g^2 \pi^4 2^{-\alpha_0 - 2} \alpha_0^2 / \Gamma^2(\tfrac{1}{2}[2 + \alpha_0 - 2\alpha(t)]) \ . \tag{3.11}$$

The triple-Pomeron coupling proper is essentially identical in the models of Veneziano and of Neveu and Schwarz although the latter model is preferred by the absence of a tachyon on the leading Pomeron trajectory at $\alpha(t) = 0$. From the study of the twisted loop in the four-point function it is known that Pomeron form factors to the Reggeon ground state are identical in the two models and are given by (2.12). Thus,

as in Eq. (2.13), factorization allows us to obtain the asymptotic discontinuity of the NS two-loop graph, Fig. 3, by multiplying (3.10) by $f_P{}^2(t)f_P(0)$.

IV. THE CENTRAL REGION

For the reasons discussed in Sec. I, it is interesting to consider the amplitude for Pomeron production in the central region. Let us begin by discussing in general terms the techniques to be used.

In the limit of large $\alpha(t)$, $\alpha(u)$, and $\alpha(s)$ with fixed $\alpha(t)\alpha(u)/\alpha(s)=\alpha(\mu_\perp{}^2)$, the general n-loop dual integrand takes the form

$$A=\int_0^\infty dx\,dy\int\left(\prod_i dz_i\right)x^{-\alpha_1(0)-1}y^{-\alpha_2(0)-1}W(z_i)e^{\alpha(t)xV_t(z_i)}e^{\alpha(u)yV_u(z_i)}e^{\alpha(M^2)xyV_M(z_i)},\qquad(4.1)$$

where z_i represents a possibly large number of other integration variables. We use the Mellin-Barnes transform to write

$$e^{\alpha(M^2)xyV_M(z_i)}=\int_{-i\infty}^{+i\infty}\frac{dn}{2\pi i}\,\Gamma(-n)[-\alpha(M^2)xyV_M(z_i)]^n.\qquad(4.2)$$

In this form the missing-mass discontinuity is clearly

$$\mathrm{Disc}\,A=\int_{-i\infty}^{+i\infty}\frac{dn}{2\pi i}\frac{[\alpha_M{}^2]^n}{\Gamma(n+1)}\int_0^\infty dx\,dy\int\prod_i dz_i\;x^{n-\alpha_1(0)-1}y^{n-\alpha_2(0)-1}$$

$$\times W(z_i)[V_M(z_i)]^n\,\theta(V_M(z_i))e^{\alpha(t)xV_t(z_i)}e^{\alpha(u)yV_u(z_i)}.\qquad(4.3)$$

If $V_t(z_i)$ and $V_u(z_i)$ change sign in the integration region, the integral defines the amplitude in the region of large imaginary α_t and α_u. Furthermore, as is clear from Eq. (4.1), the integral is well defined for $\alpha_i(0)$ negative, i.e., to the left of the n-plane contour. In the limit of large imaginary α_t and α_u the x and y integrations can be done yielding

$$\lim_{\alpha_t,\,\alpha_u\to\infty}\mathrm{Disc}\,A\sim(-\alpha_t)^{\alpha_1(0)}(-\alpha_u)^{\alpha_2(0)}\int_{-i\infty}^{+i\infty}\frac{dn}{2i}\frac{\Gamma(n-\alpha_1(0))}{\Gamma(n+1)}\Gamma(n-\alpha_2(0))\left[\frac{\alpha(M^2)}{\alpha(t)\alpha(u)}\right]^n$$

$$\times\int\left(\prod_i dz_i\right)W(z_i)[V_M(z_i)]^n[V_t(z_i)]^{\alpha_1(0)-n}[V_u(z_i)]^{\alpha_2(0)-n}.\qquad(4.4)$$

Since in the central region $tu/M^2=\mu_\perp{}^2$, we see the general factorization into a double-Regge behavior times a function of $\mu_\perp{}^2$. The problem is then to determine at least the asymptotic behavior of the $\mu_\perp$ dependence. To accomplish this one uses the inverse transform of (4.2),

$$[\alpha(\mu_\perp{}^2)]^{-n}=\frac{[\alpha(\mu_\perp{}^2)]^{-c}}{\Gamma(n-c)}\times\int_0^\infty dy\,e^{-y\,\alpha(\mu_\perp{}^2)}y^{n-c-1}.\qquad(4.5)$$

Then after amputating the Regge factors in (4.4) the $\mu_\perp$ dependence takes the form

$$f(\mu_\perp{}^2)=[\alpha(\mu_\perp{}^2)]^{-c}\int_0^\infty dy\,e^{-y\alpha(\mu_\perp{}^2)}H(y),\qquad(4.6)$$

with

$$H(y)=\int_{-i\infty}^{+i\infty}\frac{dn}{2i}\frac{\Gamma(n-\alpha_1(0))}{\Gamma(n+1)}y^{n-c-1}\times G(n)\frac{\Gamma(n-\alpha_2(0))}{\Gamma(n-c)},\qquad(4.7)$$

$$G(n)=\int\prod_i dz_i\,W(z_i)[V_M(z_i)]^n[V_t(z_i)]^{\alpha_1(0)-n}\times[V_u(z_i)]^{\alpha_2(0)-n}.\qquad(4.8)$$

In (4.6), c is any convenient constant. From Eq. (4.6) it is clear that as $\alpha(\mu_\perp{}^2)$ becomes large the integral is dominated by the smallest value of y for which $H(y)$ is nonzero. If near $y=0$, $H(y)$ behaves as

$$\lim_{y\to0}H(y)\sim ay^b,\qquad(4.9)$$
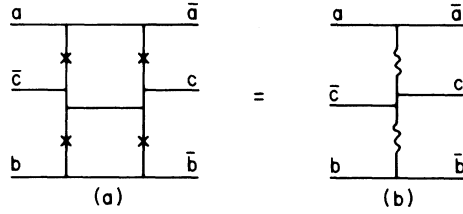
FIG. 5. Two-loop duality graph for particle production in the central region via double-Pomeron exchange. Each Reggeon propagator contributes one integration variable and each Pomeron propagator two integration variables to the dual integrand.

FIG. 6. Pomeron production in the central region.

then $f(\mu_\perp^2)$ is power behaved,

$$\lim_{\mu_\perp^2 \to \infty} f(\mu_\perp^2) \sim a\Gamma(b+1)[\alpha(\mu_\perp^2)]^{-b-1-\alpha_2(o)} . \quad (4.10)$$

If on the other hand $H(y)$ is zero in a neighborhood of $y = 0$ and behaves instead as

$$H(y) = \theta(y - y_0)[a(y - y_0)^b + \cdots], \quad (4.11)$$

then there is an exponential $\mu_\perp$ dependence,

$$\lim_{\mu_\perp^2 \to \infty} f(\mu_\perp^2) \sim a\Gamma(b+1)[\alpha(\mu_\perp^2)]^{-b-1-\alpha_2(o)}$$
$$\times e^{-y_0\alpha(\mu_\perp^2)} . \quad (4.12)$$

The behavior of $H(y)$ near $y = 0$ is determined by the pole structure of $G(n)$. As $y \to 0$ the integrand in (4.7) is exponentially damped for $\mathrm{Re}\, n \to +\infty$. Therefore, we may close the contour to the right in Eq. (4.7). If $G(n)$ has no poles to the right $H(y)$ is zero below some finite y_0 and takes the form
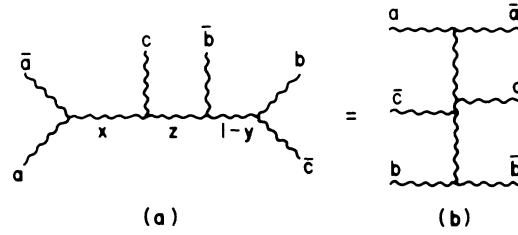
(4.11). If $G(n)$ has poles to the right, one has the case (4.9).

In all of the dual amplitudes investigated previously, i.e., in the dual Born-term calculation and in the case of the twisted or untwisted single-loop graphs, $H(y)$ has been proportional to $\theta(y - 4)$, leading to the asymptotic behavior

$$f(\mu_\perp^2) \to e^{-4\alpha' \mu_\perp^2} , \quad (4.13)$$

with α' the Reggeon slope, 0.9 GeV^{-2}.

We proceed now to apply this analysis to the Pomeron six-point function. In addition to its value in its own right the amplitude may provide the first clue to the $P_\perp$ dependence of the topologically similar two-loop graph, Fig. 5, for particle production in the central region via double-Pomeron exchange. That is, in Fig. 5 and in the present amplitude, the produced particle is quark-line disconnected from both target and projectile.

Since the Pomeron amplitudes are totally symmetric, graphs with different ordering of the external particles are fully equivalent. Nevertheless for convenience we prefer to analyze the integral form corresponding to the ordering of Fig. 6:

$$A_6 = g^8 \int d^2x\, d^2y\, d^2z\, |xy|^{-\alpha_0-2} |z|^{-\alpha(-k_c^2)-2} |1-x|^{-\alpha_t-2}$$

$$\times |1-y|^{-\alpha_u-2} |1-z|^{-\alpha_u-2} |1-z(1-y)|^{\alpha_u+2} |1-xz|^{-\alpha(s)-2} |1-xz(1-y)|^{\alpha(s)+2} . \quad (4.14)$$

The integral diverges at the origin in x, y, and z unless it is evaluated with α_0 and $\alpha(-k_c^2)$ negative and analytically continued afterwards. Kinematically,

$$\alpha(s) = \alpha(M^2) - \alpha(t) - \alpha(u) = \alpha(t)\alpha(u)/\alpha(\mu_\perp^2) , \quad (4.15)$$

and in the central region

$$1 \ll -\alpha_t, \quad -\alpha_u \ll \alpha(M^2) . \quad (4.16)$$

For large α_u, α_t the integral is dominated by the region near $x, y \approx 0$. Expanding the integrand of Eq. (4.14) about that region gives us

$$\lim_{\alpha_t, \alpha_u \text{ large}} A_6 = g^8 \int d^2x\, d^2y\, d^2z\, |xy|^{-\alpha_0-2} |z|^{-\alpha(-k_c^2)-2} e^{\alpha_t \mathrm{Re}\, x}\, e^{\alpha_u \mathrm{Re}[y/(1-z)]}\, e^{\alpha_M^2 \mathrm{Re}\, xyz} . \quad (4.17)$$

Proceeding as in (4.2) and (4.3) the discontinuity of A_6 is

$$\text{Disc}\,A_6 = g^8 \int_{-i\infty}^{+i\infty} \frac{dn}{2i\,\Gamma(n+1)} \int d^2x\,d^2y\,d^2z\,(\alpha_u 2\text{Re}xyz)^n\,\theta(\text{Re}xyz)|\,xy|^{-\alpha_0 - 2}|\,z|^{-\alpha(-k_c^2)-2}e^{\alpha_t \text{Re}x}e^{\alpha_u \text{Re}\,[y/(1-z)]}$$

(4.18)

We now make the transformation

$$y = y'(1-z), \quad d^2y = d^2y'|\,1-z|^2$$

(4.19)

and perform the integrations over the magnitudes of x and y' as in (4.4):

$$\text{Disc}\,A_6 = (-\alpha_t)^{\alpha_0}(-\alpha_u)^{\alpha_0}f(\mu_\perp^2)\,,$$

(4.20)

with

$$f(\mu_\perp^2) = g^8 \int_{-i\infty}^{+i\infty} \frac{dn}{2i}\,\frac{\Gamma^2(n-\alpha_0)}{\Gamma(n+1)}\,[\,\alpha(\mu_\perp^2)]^{-n}[\text{Re}e^{i(\omega+\phi)}z(1-z)]^n$$

$$\times\,\theta(\text{Re}e^{i(\omega+\phi)}z(1-z))|\,z|^{-\alpha(-k_c^2)-2}|\,1-z|^{-\alpha_0}(\cos\omega\cos\phi)^{\alpha_0 - n}\,d^2z\,d\omega\,d\phi\,.$$

(4.21)

We are now free to continue $\alpha(-k_c^2)$ and the Pomeron intercept α_0 to positive values providing we distort the n-plane contour so that $\alpha(-k_c^2)$ and α_0 continue to lie to the left of the contour. We apply the transform (4.5) and recover the general form (4.6) and (4.7) with $\alpha_1(0) = \alpha_2(0) = \alpha_0$ and

$$G(n) = g^8 \int d^2z\,d\phi\,d\omega\,\theta(\text{Re}e^{i(\omega+\phi)}z(1-z))[\text{Re}e^{i(\omega+\phi)}z(1-z)]^n|\,z|^{-\alpha(-k_c^2)-2}|\,1-z|^{-\alpha_0}(\cos\omega\cos\phi)^{\alpha_0 - n}\,.$$

(4.22)

The nature of the asymptotic behavior in $\mu_\perp^2$ is determined by whether or not there are n-plane poles in $G(n)$ to the right of the contour, i.e., for positive values of $n - \alpha_0$. We answer this question negatively in the dual-model ghost-free configuration $\alpha_0 = 2$, $\alpha_P(-k_c^2) = 0$. The behavior of $f(\mu_\perp^2)$ in this configuration is important to the self-consistent exploration of the dual-resonance model, although from a phenomenological point of view, it may be interesting to ask what $\mu_\perp$ dependence is defined by the same integrals with $\alpha_0 = 1$.

In the ghost-free configuration the integral is simplified by the substitution

$$z = \tfrac{1}{2}[1 + (1-z')^{1/2}]\,,$$

(4.23)

$$G(n) = 2g^8 \int \frac{d^2z\,d\phi\,d\omega}{|\,1-z||\,z|^2}\,(\tfrac{1}{4}\text{Re}ze^{i\omega+\phi})^n\,\theta(\text{Re}ze^{i\omega+\phi})(\cos\omega\cos\phi)^{2-n}\,.$$

(4.24)

If we write $z = ve^{i\theta}$, the integral over v is a Legendre function,

$$G(n) = 2g^8\Gamma(n,1-n)\int_{-\pi}^{\pi} d\omega\,d\theta\,d\phi\,P_{n-1}(-\cos\theta)4^{-n}(\cos\omega + \phi + \theta)^n\,\theta(\cos\omega + \phi + \theta)(\cos\omega\cos\phi)^{2-n}\,.$$

(4.25)

Here we introduce the notation

$$\Gamma(a_1, a_2\ldots, a_k) = \prod_{i=1}^{k}\Gamma(a_i)\,.$$

(4.26)

The reality of the discontinuity is ensured by the phase convention that negative $\cos\omega$ is $e^{i\pi}|\cos\omega|$ while negative $\cos\phi$ is $e^{-i\pi}|\cos\phi|$. This is equivalent to putting $(-1)^n = \cos\pi n$ when it occurs in the last factor of (4.25). If we call the integrand of (4.25)$f(\theta, \phi, \omega)$, the angular symmetries can be exploited to write

$$G(n) = 4\int_0^{\pi} d\theta\int_0^{\pi/2} d\omega\int_{-\pi}^{\pi} d\phi[f(\theta, \phi, \omega) + f(\theta, \phi, -\omega)]\,.$$

(4.27)

We are therefore led to calculate the integral

$$I(n) = \int_{-\pi}^{\pi} d\phi(\cos\phi)^n\,\theta(\cos\phi)[(\cos\phi - \theta - \omega)^{2-n} + (\cos\phi - \theta + \omega)^{2-n}]\,.$$

(4.28)

One finds[13]

$$I(n) = \tfrac{1}{2}\pi[(2-n)\cos n\omega\cos n\theta + n\cos(n-2)\theta\cos(n-2)\omega]\,.$$

(4.29)

Hence,

$$G(n) = 4\pi g^8 4^{-n} \Gamma(n, 1-n) \int_0^\pi d\theta \int_0^{\pi/2} d\omega \, P_{n-1}(-\cos\theta)(\cos\omega)^{2-n}$$
$$\times \left[(2-n)\cos n\omega \cos n\theta + n \cos(n-2)\theta \cos(n-2)\omega \right]. \qquad (4.30)$$

The integration over ω is easily done, yielding

$$G(n) = \pi^2 g^8 2^{-n-1} \Gamma(n, 1-n) \int_0^\pi d\theta \, P_{n-1}(-\cos\theta)[(2-n)^2 \cos n\theta - n \cos(n-2)\theta]. \qquad (4.31)$$

The final integration is done by developing the Legendre function in a power series in $\cos^2(\tfrac{1}{2}\theta)$ and integrating term by term. One has

$$R(\beta) \equiv \int_0^\pi d\theta P_{n-1}(-\cos\theta) \cos\beta\theta = \frac{\pi}{\Gamma(1+\beta, 1-\beta)} \, {}_3F_2(n, 1-n, \tfrac{1}{2}, 1+\beta, 1-\beta; 1). \qquad (4.32)$$

This particular ${}_3F_2$ is expressible via Whipple's theorem in terms of products of Γ functions:

$$R(\beta) = \pi^2[\Gamma(\tfrac{1}{2}(n+1+\beta), \tfrac{1}{2}(n+1-\beta), \tfrac{1}{2}(2+\beta-n), \tfrac{1}{2}(2-\beta-n))]^{-1}. \qquad (4.33)$$

The result is

$$G(n) = \pi^{7/2} g^8 2^{-n-1} \frac{\Gamma(n)}{\Gamma(n+\tfrac{1}{2})} (2-n)^2. \qquad (4.34)$$

The poles of $G(n)$ are seen to lie to the left of the contour in the n plane. Hence we will have an exponential $P_\perp$ dependence. Substituting (4.34) into (4.7) enables us to determine the slope of the exponential,

$$H(y) = \pi^{7/2} g^8 2^{-2-c} \int_{-i\infty}^{+i\infty} \frac{dn}{2i} (y/2)^{n-c-1} \frac{\Gamma^2(n-2)\Gamma(n)(2-n)^2}{\Gamma(n-c)\Gamma(n+1)\Gamma(n+\tfrac{1}{2})}. \qquad (4.35)$$

The parameter c is most conveniently chosen to be unity. Then

$$H(y) = \pi^{7/2} g^8 2^{-3} \int_{-i\infty}^{+i\infty} \frac{dn}{2i} (y/2)^{n-2} \frac{\Gamma(n-1)\Gamma(n)}{\Gamma(n+1)\Gamma(n+\tfrac{1}{2})}. \qquad (4.36)$$

We see that for $y < 2$ the integrand is exponentially damped as $\text{Re}\,n \to +\infty$. Therefore in this case the contour can be closed to the right and the integral vanishes since there are no poles to the right. If $y > 2$ the integrand can be closed to the left giving us the residue of the double pole at $n=0$ and the single poles at other integer values of $1-n$. One finds

$$H(y) = \tfrac{1}{4}\pi^4 g^8 (\tfrac{1}{2}y)^{-2}\{[\tfrac{1}{2}y(\tfrac{1}{2}y-1)]^{1/2} - \ln[(\tfrac{1}{2}y)^{1/2} + (\tfrac{1}{2}y-1)^{1/2}]\}\theta(y-2).$$

Near $y = 2$, $H(y)$ behaves as

$$H(y) = \frac{\pi^4 g^8}{12\sqrt{2}} \, \theta(y-2)[(y-2)^{3/2} + O((y-2)^2)]. \qquad (4.37)$$

The $\mu_\perp$ dependence is

$$f(\mu_\perp^2) = [\alpha(\mu_\perp^2)]^{-1} \int_0^\infty dy \, e^{-y\alpha(\mu_\perp^2)} H(y). \qquad (4.38)$$

For large $\mu_\perp$ we may use the first term in (4.37) to write

$$\lim_{\mu_\perp \to \infty} f(\mu_\perp^2) \sim g^8 \frac{\pi^4}{12\sqrt{2}} \Gamma(\tfrac{5}{2})[\alpha(\mu_\perp^2)]^{-7/2} e^{-2\alpha_P(\mu_\perp^2)}. \qquad (4.39)$$

This compares with the following $\mu_\perp$ dependence of normal particle production in the dual Born term[14]

$$\lim_{\mu_\perp \to \infty} f(\mu_\perp^2) \sim g^4 \pi \Gamma(\tfrac{1}{2})[\alpha_R(\mu_\perp^2)]^{-7/2} e^{-4\alpha_R(\mu_\perp^2)}. \qquad (4.40)$$

The difference in slope between (4.39) and (4.40) comes not only because of the smaller slope of the Pomeron trajectory along the lines suggested in Ref. 11 but also because the numerical coefficient is halved in the case of Pomeron production.
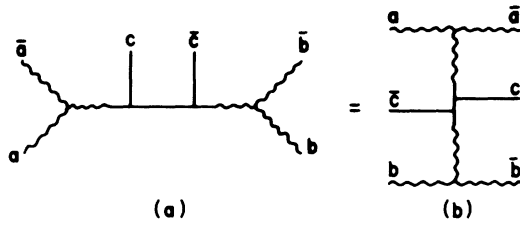
FIG. 7. Particle production by external Pomerons in the central region, allowing the extraction of the Pomeron-Pomeron-particle-particle coupling of Fig. 5.

V. CONCLUSION

We have extracted the triple-Pomeron couplings corresponding to the dual models of Veneziano and Neveu and Schwarz. In the case of physical intercepts, these are shown to be nonvanishing at t = 0 contrary to expectation in the case of the Neveu-Schwarz model. The mechanism discussed by Lovelace[7] applies only to the first term in the large square brackets of Eq. (3.9). The triple couplings (2.11) and (3.11) have double right-signature nonsense zeros given by the inverse Γ functions, at $\alpha_0 - 2\alpha(t) = -2k$, $k = 1, 2, 3, \ldots$. The wrong-signature nonsense zeros found in the dual Born term and originally thought to be responsible for a vanishing of[4,5] $g_{PPP}(0)$ do not occur. This is in line with the insight gained by studying twisted graphs in ϕ^3 field theory.[6] The fact that the right-signature nonsense zero in the triple-Pomeron coupling is a second-order zero is an unexpected result whose possible significance is as yet unclear. Similarly, it is not clear what significance should be attached to the fact that the right-signature nonsense zeros do produce a zero at t = 0 in the case of the unphysical intercept (α_0 = 2) of the ghost-free dual models. It is not inconceivable that this plays a role in the renormalization of the dual-Reggeon calculus.

One might also note in passing that if the critical intercept of the Neveu-Schwarz model were α_0 = $\frac{4}{3}$ the triple-Pomeron coupling would vanish identically and not just at t = 0. This can be seen from Eq. (3.9).

Finally we remark that while the Veneziano model suffers from the Pomeron tachyon pole at $\alpha_P(t) = 0$ [Eq. (2.10)], the Neveu-Schwarz amplitude [Eq. (3.10)] is free of this problem and can be taken as a phenomenological model with no obvious defects if one inserts physical intercepts into the final form.

In the central region the $\mu_\perp$ dependence of

Pomeron production falls asymptotically as $\exp[-2\alpha_P(\mu_\perp^2)]$ or $\exp[-\alpha_R(\mu_\perp^2)]$ in view of the dual Pomeron having half the slope of the Reggeon trajectory. This compares with an $\exp[-4\alpha_R(\mu_\perp^2)]$ asymptotic form for particle production via secondary Regge trajectory exchange.

With regard to the experimental search for gluon states one can make the following comments: If the behaviors (4.39) and (4.40) were dominant for Pomeron and particle production, respectively, at high $P_\perp$, the result would be a dramatic increase in the Pomeron-to-normal-particle ratio for increasing $P_\perp$. Invariant-mass plots of high-$P_\perp$ isospin-zero multibody states would then be sensitive to Pomeron resonances. In actuality, however, it is known that another mechanism, usually described by hard-scattering models, is effective at very high $P_\perp$, leading to a power-law behavior. Thus our results would, at best, suggest some enhanced Pomeron production at intermediate values of $P_\perp$, say between one and two GeV.

The present analysis represents the first dual production amplitude found to have a $\mu_\perp$ dependence less steep than $\exp(-4\mu_\perp^2)$. This latter dependence was found in the dual Born-term amplitudes,[14] in the single-planar-loop amplitude,[15] and in the single-twisted-loop amplitude involving single-Pomeron exchange.[16] The present work therefore provides the first indication that the $P_\perp$ dependence of the dual model may in fact be softened by the higher-order terms of the perturbation expansion.

The next step in this program would be the analysis of the single-Reggeon production via double-Pomeron exchange corresponding to the two-loop graph of Fig. 5. This amplitude is given by a nine-dimensional integral complicated by the presence of many Regge cuts.

Again we can extract the relevant information by considering amplitudes with external Pomerons. That is, the central-region Pomeron-Pomeron-particle-particle coupling of Fig. 5(b) is obtainable via factorization from the amplitude for Pomeron plus Pomeron goes to particle plus anything, as shown in Fig. 7.

These hybrid amplitudes with external Pomerons and Reggeons were first written down by one of us[17] and independently by Ademollo et al.[18] The resulting amplitude corresponding to Fig. 7 is a seven-dimensional integral, meromorphic in the J plane. Consequently, one might expect considerable simplification relative to the direct calculation of Fig. 5. The remaining triple couplings $g_{PPR}(t)$ and $g_{PRP}(t)$ could also be extracted from this amplitude, which will be the object of a future study.

*Equipe de Recherche associée au C. N. R. S.

[1] V. N. Gribov and A. A. Migdal, Yad. Fiz. 8, 1002 (1968) [Sov. J. Nucl. Phys. 8, 583 (1969)].

[2] J. B. Bronzan, Phys. Rev. D 6, 1130 (1972).

[3] A. A. Migdal, A. M. Polyakov, and K. A. Ter-Martirosyan, Phys. Lett. 48B, 239 (1974); H. D. I. Abarbanel and J. B. Bronzan, Phys. Rev. D 9, 2397 (1974); Phys. Lett. 48B, 345 (1974).

[4] P. V. Landshoff and W. J. Zakrzewski, Nucl. Phys. B12, 216 (1969); D. Gordon and G. Veneziano, Phys. Rev. D 3, 2116 (1971).

[5] S.-J. Chang, D. Gordon, F. E. Low, and S. B. Treiman, Phys. Rev. D 4, 3055 (1971).

[6] D. Gordon, Phys. Rev. D 5, 2102 (1972); A. H. Mueller and T. L. Trueman, ibid. 5, 2115 (1972).

[7] C. Lovelace, Phys. Lett. 40B, 551 (1972).

[8] M. A. Virasoro, Phys. Rev. 177, 2309 (1969); J. A. Shapiro, Phys. Lett. 33B, 361 (1970).

[9] J. Schwarz, Nucl. Phys. B46, 61 (1972).

[10] R. Aldrovandi and A. Neveu, Orsay report, 1972 (unpublished).

[11] J.-P. Ader and L. Clavelli, Phys. Lett. 66B, 97 (1977).

[12] For a discussion of these boundary conditions see R. C. Brower, C. E. DeTar, and J. H. Weis, Phys. Rep. 14C, 259 (1974).

[13] See integral 3.252.14 of I. S. Gradshteyn and I. M. Ryzhik, Tables of Integrals, Series, and Products (Academic, New York, 1965).

[14] M. A. Virasoro, Phys. Rev. D 3, 2834 (1971).

[15] V. Alessandrini and D. Amati, report (unpublished).

[16] V. Alessandrini and D. Amati, Nuovo Cimento 13A, 663 (1973); J.-P. Ader and L. Clavelli, Nucl. Phys. B133, 327 (1978).

[17] L. Clavelli, Phys. Rev. D 9, 3449 (1974).

[18] M. Ademollo, A. D'Adda, R. D'Aurio, E. Napolitano, P. DiVecchia, P. Gliozzi, and S. Sciuto, Nucl. Phys. B77, 189 (1974).
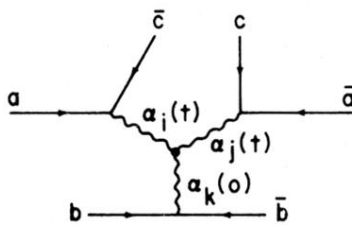
FIG. 1. Triple–Regge graph for the process $a + b \rightarrow c$ + anything.
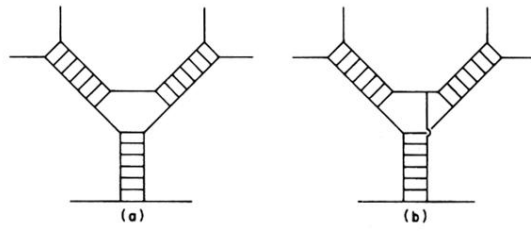
FIG. 2. Ladder graphs in ϕ^3 field theory showing triple-Regge behavior with (a) planar coupling and (b) nonplanar coupling.
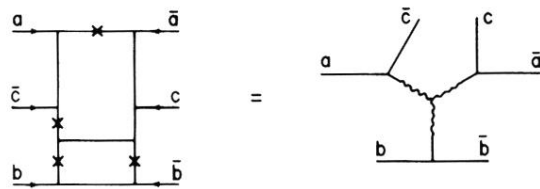
FIG. 3. Two-loop duality graph containing the triple-Pomeron coupling. Wavy lines represent Pomerons, straight lines represent Reggeons. The effect of the twists is to prevent particles separated by a Pomeron from exchanging quarks.
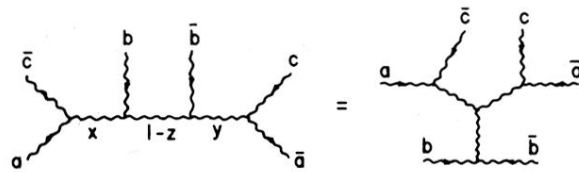
FIG. 4. Tree graph for external Pomerons allowing extraction by factorization of the triple-Pomeron coupling.
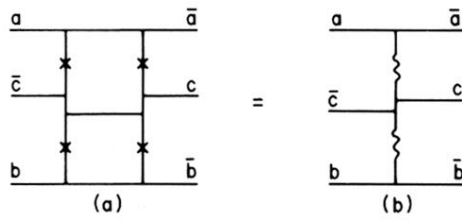
FIG. 5. Two-loop duality graph for particle production in the central region via double-Pomeron exchange. Each Reggeon propagator contributes one integration variable and each Pomeron propagator two integration variables to the dual integrand.
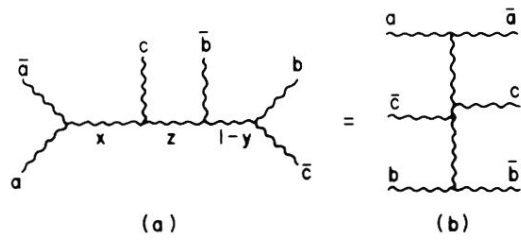
FIG. 6. Pomeron production in the central region.

FIG. 7. Particle production by external Pomerons in the central region, allowing the extraction of the Pomeron-Pomeron-particle-particle coupling of Fig. 5.